Journal of Thermal Analysis and Calorimetry, Vol. 97 (2009) 2, 541–546

AMORPHOUS PHASE DYNAMICS AT THE GLASS TRANSITION IN DRAWN SEMI-CRYSTALLINE POLYESTER
DMA and TMDSC comparative studies

N. Delpouve[*]*, C. Lixon, A. Saiter, E. Dargent and J. Grenet*

Laboratoire PBS, FRE 3101, LECAP, Institute for Materials Research. Université de Rouen, Faculté des Sciences, Avenue de l'Université BP 12, 76801 Saint Etienne du Rouvray, France

Temperature modulated differential scanning calorimetry (TMDSC) and dynamic mechanical analysis (DMA) are used to calculate cooperative rearranging region (CRR) average sizes for drawn poly(ethylene terephthalate) (PET) with different draw ratios (λ) ranging from λ=1 to 4, according to Donth's approach. It is shown for both studies that the CRR size decreases when λ increases, due to the amorphous phase confinement by the crystals generated during the drawing. However, differences observed between the values calculated from TMDSC and DMA investigations are explained by the differences between a mechanical uniaxial dynamic solicitation (DMA) or a thermal solicitation (TMDSC) in terms of cooperative rearrangements at the glass transition.

Keywords: *CRR, DMA, drawing, PET, TMDSC*

Introduction

Temperature modulated differential scanning calorimetry (TMDSC) is a tool providing a lot of useful applications among which the possibility to separate the thermal events related to the heat capacity (C_p) and the kinetic events [1, 2]. Thus, it is commonly used to investigate the different phenomena occurring around the glass transition, and particularly concerns the amorphous phase rearrangement when the material moves from the liquid-state down to the glassy one. Adam and Gibbs firstly introduced the cooperative rearranging region (CRR) concept [3], defined as a subsystem which can rearrange into another configuration independently of its environment, and appears during the cooling in the glass transition temperature region upon a sufficient thermodynamic fluctuation. In each subvolume, the density ρ, the temperature T, the entropy S and the energy E are somewhat different, and the mean square fluctuations $<\Delta\rho^2>$, $<\Delta T^2>$, $<\Delta S^2>$ and $<\Delta E^2>$ are given by standard relations of statistical thermodynamic [4]. The main idea developed by Donth *et al.* [5–7] has been to relate these statistical thermodynamic relations to the width of relaxation time distribution of the so-called α process. Each subvolume can be then considered as a thermodynamic system in metastable equilibrium with fluctuating variables having a gaussian distribution, and has its own glass transition temperature T_α and its own relaxation time τ. Thus, the relaxation time distribution is related to the glass transition one where $<T_\alpha>$ is assumed to be the conventional glass transition temperature of the sample.

In this approach [8], the characteristic volume of cooperativity at T_α noted $\xi^3_{T_\alpha}$, and the number of monomer units in the CRR noted N_α, can be estimated from the two following equations:

$$\xi^3_{T_\alpha} = \frac{\Delta(1/C_v)}{\rho(\delta T)^2} k_B T_\alpha^2 \quad (1)$$

$$N_\alpha = \frac{\rho N_A \xi^3_{T_\alpha}}{M_0} \quad (2)$$

with N_A the Avogadro number, $(\delta T)^2$ the mean square temperature fluctuation related to the dynamic glass transition of a CRR [8–10], T_α the glass transition temperature, k_B the Boltzmann constant, ρ the polymer density, C_v the heat capacity at constant volume and M_0 the molar mass of a monomer unit. The approximation for the calculation of the characteristic cooperativity volume $\xi^3_{T_\alpha}$ from Eq. (1) neglects the difference between the heat capacity step variations at constant pressure and at constant volume, and the step of reciprocal specific heat capacity can be estimated from:

$$\Delta(1/C_v) \approx \Delta(1/C_p) = (1/C_p)_{glass} - (1/C_p)_{liquid} \quad (3)$$

Many recent works on the CRR size determination from Donth's approach exist in the literature [11–13] and it has been proved that CRR average sizes can be provided using TMDSC [14]. For exam-

* Author for correspondence: nicolas.delpouve@etu.univ-rouen.fr

1388–6150/$20.00

Akadémiai Kiadó, Budapest, Hungary
Springer, Dordrecht, The Netherlands

ple, Xia *et al.* have shown the two-dimensional confinement influence on the CRR average size decrease in polymer/clay nanocomposites [15]. Very recently we have correlated the crystallinity degree (spherulitic crystallization) with the CRR average size in poly(*L*-lactic acid) (PLLA) samples [16, 17].

As proposed by Donth *et al.* [18], the mean temperature fluctuation can be estimated from any loss peak depending on the experimental technique used: for example from the dynamic heat capacity C'' in TMDSC, the dielectric function ε" in dielectric relaxation spectroscopy (DRS) or the viscous modulus *E*" in dynamic mechanical analysis (DMA). So, our idea is to calculate the CRR average sizes from DMA investigations and to compare the results to those obtained by TMDSC analysis on the same samples.

To reach this goal, we have chosen to work on poly(ethylene terephthalate) (PET) samples drawn above the glass transition temperature. It has been shown previously [19, 20], that under these conditions, and above a critical draw ratio value noted λ_c, a strain induced crystallization (SIC) phase with a weak fibrillar texture appears in PET. So, in this work, we give new results on the evolution of CRR average sizes at glass transition for strain induced semi-crystalline microstructure.

Experimental

Initial PET material is obtained from a film of 500 μm thickness extruded by Carolex Co. The number-average molecular mass is $\overline{M}_n$=31.000 g mol^{-1} and the mass-average molecular mass is $\overline{M}_w$=62.000 g mol^{-1}. The polymer amorphous phase density is ρ=1.336 g cm^{-3} and the molar mass of one monomer unit is M_0=192 g mol^{-1}. The initial film is isotropic and practically amorphous (not fully) according to birefringence, density and X ray diffraction measurements [15]. Drawn semi-crystalline samples are obtained from the following procedure. Before the drawing period, the films are kept in the heating chamber of a tensile machine at T=100°C for 15 min, allowing a homogenous temperature distribution. Then, the films are uniaxially drawn at a strain rate of $\dot{\varepsilon}$=0.14 s^{-1} in the tensile machine from an initial length l_i to a final length l_f. The heating chamber temperature (100°C) chosen between the glass transition temperature and the cold crystallisation temperature of PET allows homogeneous drawing and avoids thermal crystallisation. After drawing the material is cold air-quenched down to room temperature in order to freeze in its structural state. Finally, as shown in Fig. 1, different samples are cut and the draw ratio λ, equal to the ratio of the extended length over the original length, varies from 1 to 4. Undrawn and drawn

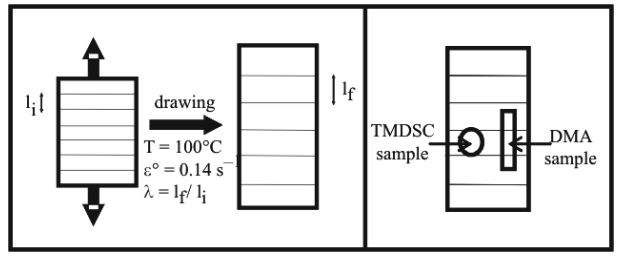

Fig. 1 Scheme of a – the PET film drawing and b – example of samples used for the two analysis. Lines are drawn with an ink to measure locally the draw ratio λ:l_i is the initial length and l_f, the final length. The incertitudes on λ are considered as lower than ±0.1

samples are stored before experiments under vacuum in the presence of P_2O_5 at 20°C in order to avoid moisture sorption.

Two different experimental techniques are used in this work: TMDSC and DMA. Firstly, the samples are analyzed by TMDSC performed on a TA Instruments apparatus (DSC 2920). Calibration in temperature and energy is normally carried out using standard values of indium, and the specific heat capacities for each sample are measured using sapphire as a reference. The sample masses are chosen to be similar to the sapphire sample mass, i.e. approximately 20 mg. The TMDSC experiments are performed with an oscillation amplitude of 0.318°C, an oscillation period of 60 s and with a heating rate of 2°C min^{-1}. From TMDSC analysis, two signals are first obtained: the modulated heat flow and the modulated heating rate, from which we can calculate all other data. We use the total heat flow, corresponding to the average modulated heat flow to calculate crystallinity ratio X_c. Concerning the CRR size calculation, we need the heat capacity C_p considered as a complex quantity C^* [21] and obtained by TMDSC [22] with the two first signals by Fourier transform. Indeed, from the ratio between the amplitude of the modulated heat flow A_q and the amplitude of the modulated heating rate A_β, it is possible to extract the C^* signal according to Eq. (4):

$$|C^*| = \frac{A_q}{A_\beta}\frac{1}{m} \tag{4}$$

where m is the sample mass. Then, we are interested in the C^* in-phase component noted C' and out-of-phase component noted C", from which the average size of CRR and the average number of monomer units per CRR are calculated. As explained by Weyer *et al.* [23], the time-consuming heat transfer into the sample needs time and yields a phase angle δ between the calorimeter response function (i.e. the heat flow) and the time derivative of the modulated temperature program. The first part of this phase an-

gle δ_{ht} is due to the heat transfer in the sample and is strongly dependant on the thermal contact between the sample and its support, and on the heat conductance of the sample itself. δ_{ht} can be estimated as:

$$\delta_{ht} = \frac{\omega|C^*|}{K} \quad (5)$$

with ω the angular frequency and K the heat conductance of the heat flow path between the sample and its support. As δ_{ht} is a function of the complex apparent heat capacity, it is taken into account during the sapphire calibration.

In the case of relaxation processes, like glass transition, an additional phase angle δ_s caused by the relaxation process can be observed [24]. This phase angle δ_s is related to sample properties and not to heat transport processes. Thus, the two components C' and C'' are calculated according to the following equations:

$$C' = |C^*|\cos\delta_s \quad (6)$$

$$C'' = |C^*|\sin\delta_s \quad (7)$$

where C^* and δ_s are functions of temperature and frequency.

In a second way, DMA measurements are performed on TA instrument (Q800) in the tension mode. The samples are then placed in tension between a fixed clamp and a moveable one. Calibrations were made in accordance with TA procedures. In oscillation experiments, the temperature of the measurement is restricted to a range from 40 to 150°C. The other experimental parameters are the following: heating rate of 2°C min^{-1} (similar to TMDSC), air atmosphere, amplitude of 15 μm and frequency of 1 Hz. In this case, the measure is performed in the drawing direction. A decrease of the storage modulus during the glass transition is observed (not shown here) and we use the loss modulus signal, describing the energy dissipation into heat when the material is deformed, to obtain the mean temperature fluctuation (δT) related to the dynamic glass transition of one CRR. The peak maximum temperature is assumed to be the α process temperature (T_α) [25, 26]. Thus, $\xi^3_{T_\alpha}$ can be calculated by means of these two parameters, and of $\Delta(1/C_v)$ determinated with the C' signal on TMDSC.

Results and discussion

The values of the initial crystallinity degree X_c are calculated on total heat flow curves in TMDSC (not shown here) [27] by:

$$X_c = \frac{\Delta H_f - \Delta H_c}{\Delta H_f^0} \quad (8)$$

where ΔH_f is the measured fusion enthalpy, ΔH_f^0 is the calculated fusion enthalpy of a wholly crystalline material (ΔH_f^0=140 J g^{-1}) [28] and ΔH_c is the exothermic peak enthalpy of cold crystallization obtained during the TMDSC runs. These X_c values are given in Table 1 and presented on Fig. 2 as a function of the draw ratio.

Before the drawing, the material is weakly crystalline (X_c=7%), then the crystallinity degree increases slowly until a draw ratio of λ=2.4 is reached, and finally, from λ=2.4 to 4, X_c increases quickly till a value of 35%. So, as put also in evidence from X-ray analysis in a previous work [18], a Strain-Induced Crystalline (SIC) phase appears during the drawing.

Figure 3 gives an example of C' and C'' curves obtained by TMDSC for a draw ratio λ=1 and describes the procedure to calculate the different parameters in the Eq. (1): T_α is the C' maximum temperature, $C_{p_{glass}}$ and $C_{p_{liquid}}$ are determined at T_α in Eq. (1) and $2\delta T$ is the C'' half-high width.

Table 1 Experimental parameters obtained from TMDSC investigations on drawn PET with different draw ratios ranging from λ=1 to 4: X_a: relaxing material quantity; X_c: crystallinity degree

λ	X_a/%	X_c/%
1.0	60±8	7±5
1.2	67±8	8±5
1.4	73±8	9±5
1.6	75±8	8±7
2.0	77±8	10±7
2.4	64±8	13±8
3.0	31±8	21±8
4.0	35±8	35±9

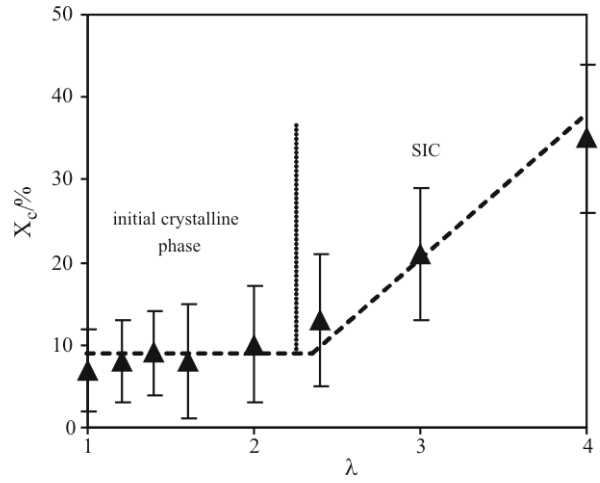

Fig. 2 Crystallinity degree X_c evolution in function of draw ratio measured by TMDSC on the Total Heat Flow signal and calculated from Eq. (8). The uncertainties are calculated by drawing the baselines so as to obtain enthalpy values the most extreme possible

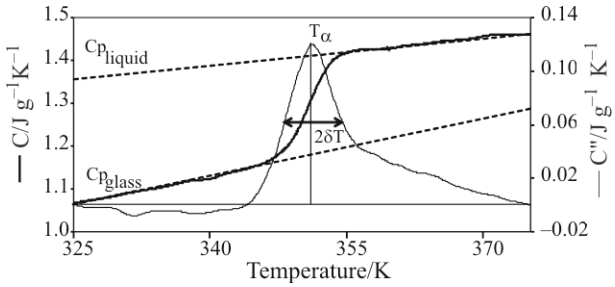

Fig. 3 Example of *C*' and *C*" curves obtained by TMDSC during heating on a PET sample with a draw ratio λ=1, to explain the determination of the quantities needed for the calculation of the characteristic cooperativity volume at the glass transition $\xi^3_{T_\alpha}$

Then, as the material could have various X_c, it is important to normalize the *C*' signal to the quantity which relaxes at the glass transition: X_a.This quantity is calculated from the ΔC_p step data at the glass transition:

$$X_a = \frac{\Delta C_p}{\Delta C_p^0} \tag{9}$$

where ΔC_p is the thermal heat capacity step of a drawn sample at the glass transition, and ΔC_p^0 that of a 100% amorphous sample, equal to 0.40 J g^{-1} K^{-1} for PET [19]. X_a values are given in Table 1 and the uncertainties concerning $C_{p_{glass}}$ and $C_{p_{liquid}}$ asymptotes are taken as large as possible. Consequently, the values of $C_{p_{glass}}$ and $C_{p_{liquid}}$ used to calculate the CRR sizes are taken on the *C*' normalized signal. Furthermore, *C*" curves are fitted by Gaussian functions as described by many authors [29]. In DMA analysis, as shown on Fig. 4, T_α and δT are extracted from the loss modulus curve and allow us to calculate $\xi^3_{T_\alpha}$.

If we consider now the different Donth's equation (1) parameters, the T_α evolution as a function of draw ratio is presented on Fig. 5.

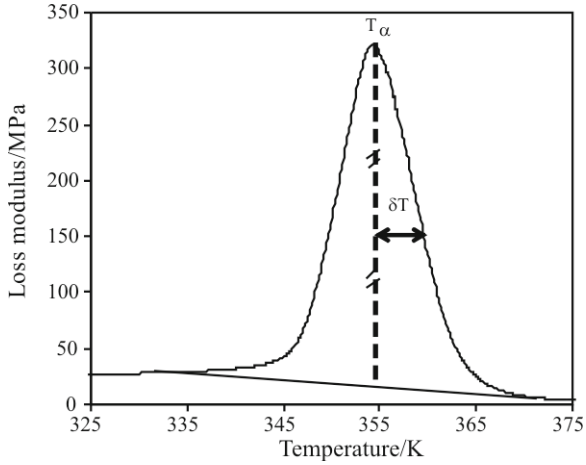

Fig. 4 Example of loss modulus spectrum obtained from DMA investigations on a PET sample with a draw ratio λ=1

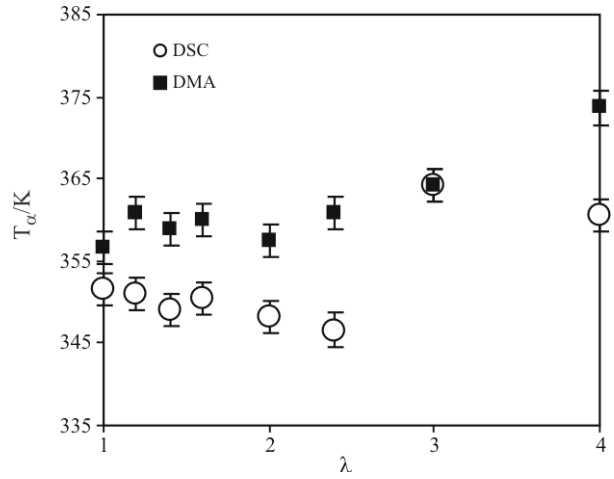

Fig. 5 Glass transition temperature T_α evolution in function of draw ratio for the two analysis techniques: DMA and TMDSC. We estimate the incertitudes on T_α around ±2 K and only linked to the error during the experimental measure

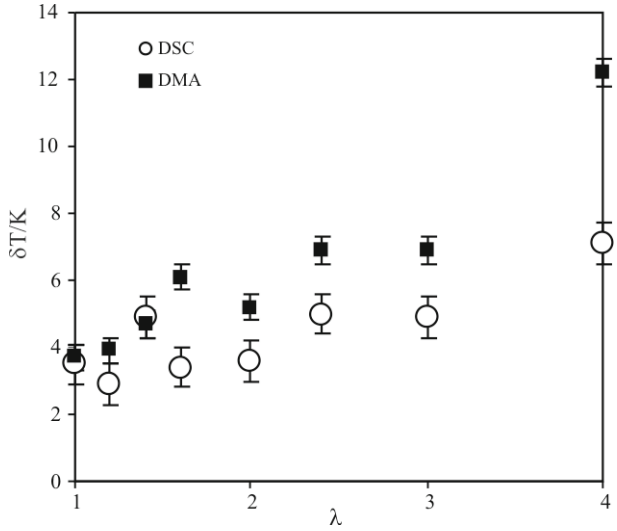

Fig. 6 Mean temperature fluctuation δT evolution in function of draw ratio for the two analysis techniques: DMA and TMDSC. The δT determination is made several times and the incertitudes after result comparison are estimated to ±0.6 K for DSC and ±0.4 K for DMA

We observe similarities between the profiles obtained by TMDSC and DMA. First the curve looks quasi constant until the draw ratio of λ=2.4 is reached. Then, T_α increases to reach its maximum value for a draw ratio of λ=4. We can see also that there exists a shift between the values resulting from the TMDSC analysis compared to these obtained by DMA analysis. The TMDSC values are significantly lower, lying from 347 to 360 K whereas DMA values vary from 357 to 373 K. This evolution follows the profile of the X_c as a function of draw ratio shown on Fig. 2. Concerning the mean temperature fluctuation presented on Fig. 6, we observe also similarities be-

tween the two curves: an increase of δT when λ increases from 1 to 4 and a shift between the values obtained by the two techniques. Indeed, δT varies from 2.9 to 7.1 K for TMDSC and from 3.7 to 12.2 K for DMA. These results are discussed below.

The crystallinity increase, due to the drawing process, induces a T_α increase [30]. Below λ=2, X_c is constant and no evolution for the glass transition temperature is observed, but for draw ratio higher than 2.4, the SIC phase appeareance causes a coupling effect with the amorphous phase revealed by the T_α increase. When the draw ratio λ=4 is reached, a fibrillar structure is obtained in the material. The amorphous phase becomes anisotropic as previously shown, by birefringence measurements [19]. It is generally stated that a T_α increase occurs in systems exhibiting strong interactions at polymer/surface [31], like crystalline ones. In our case, since polymer chains participate both to the material different phases (organized or not), the system is considered as a strongly interacting one and that partially explains the T_α increase.

Concerning the mean temperature fluctuation increase, the material becomes more crystalline after the drawing and it brings on heterogeneities in its structure inducing a widening of the relaxation time distribution. So δT increases when macromolecular orientation appears at first (till λ=2.4) and then, when crystallization occurs.

Now, Fig. 7 presents the cooperativity length ξ_{T_α} evolution as a function of draw ratio. The error bars are calculated from the generally accepted value of 10% as suggested by Hempel *et al.* [32]. We can see first that TMDSC and DMA are suitable to calculate CRR average sizes since the values obtained from the two techniques for λ=1 are the same. The overall results show then a decrease of the CRR volume $\xi^3_{T_\alpha}$

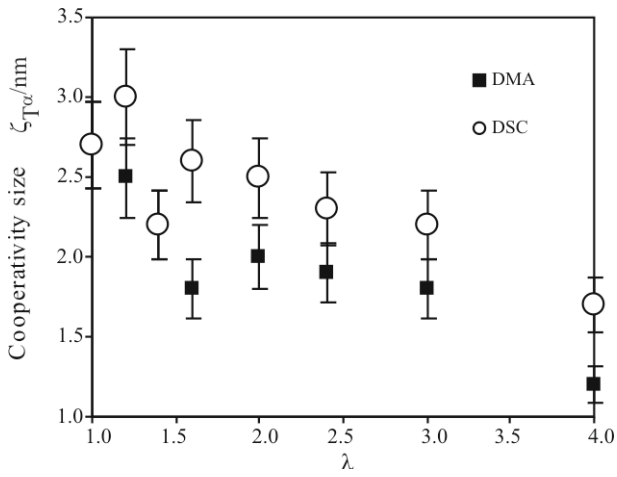

Fig. 7 CRR characteristic cooperativity length ξ_{T_α} evolution in function of draw ratio obtained from DMA and TMDSC investigations at T_α

when the draw ratio increases. From the TMDSC, CRR average size varies from 3 to 1.7 nm whereas from DMA they vary from 2.7 to 1.2 nm. These results are explained by the amorphous phase confinement by the crystals generated during the drawing. The decrease of the length becomes more important as the draw ratio increases, showing that molecular orientation can be directly related to the cooperativity length evolution.

It is previously mentioned that differences between the results obtained by TMDSC and by DMA are visible, despite the fact that their evolutions are similar. Indeed, it is well known that the glass transition can be weakly shifted between these two experimental techniques [33, 34] since a mechanical solicitation (DMA) can yield different results than a thermal solicitation (TMDSC) [35] in terms of conformational mobility [36] and cooperative rearrangements at the glass transition. Moreover, DMA results are strongly dependent on the measurement frequency [37] and we assume that the selected one is different from the frequency corresponding to the T_α measured by TMDSC. So, the variations are in range of what was expected and CRR average sizes determination by the two techniques leads to similar results.

Conclusions

This study compares the results obtained by DMA and TMDSC analyses to characterize the effect of amorphous phase confinement by SIC phase in PET. The cooperativity length is calculated with Donth's approach and the evolution is related to the draw ratio. We show that CRR average sizes decrease drastically from 2.9 to 1.5 nm when the draw ratio increases, due to the appearance and growth of crystalline phase which confines the relaxing material part. These results are related to the evolution of glass transition temperature which ranges from 352 to 367 K and of the mean temperature fluctuation which varies from 3.3 to 9.7 K. The slight variation observed between the results obtained by the two techniques is ascribed to the difference between an only thermal and a mechanical solicitation, causing changes in cooperative rearranging processes at the glass transition.

References

1 J. E. K. Schawe, Thermochim. Acta, 260 (1995) 1.
2 M. Reading and R. Luyt, J. Thermal Anal., 54 (1998) 535.
3 G. Adam and J. H. Gibbs, J. Chem. Phys., 43 (1965) 139.
4 L. D. Landau and E. M. Lifshitz, Statistical Physics, Addison-Wesley, Reading MA 1969
5 E. Donth, J. Non-Cryst. Solids, 131-133 (1991) 204.

6 C. T. Moynihan and J. Schroeder, J. Non-Cryst. Solids, 161 (1993) 148.
7 U. Mohanty, Adv. Chem. Phys., 89 (1995) 89.
8 E. Donth, J. Non-Cryst. Solids, 53 (1982) 325.
9 E. Donth, J. Polym. Sci. B, 34 (1996) 2881.
10 E. Donth, Acta Polym., 50 (1999) 240.
11 T. A. Tran, S. Saïd and Y. Grohens, Composites: Part A, 36 (2005) 461.
12 G. Dlubek, J. Non-Cryst. Solids, 352 (2006) 2869.
13 A. Saiter, H. Couderc and J. Grenet, J. Therm. Anal. Cal., 88 (2007) 483.
14 E. Hempel, A. Huwe, K. Otto, F. Janowski, K. Schröter and E. Donth, Thermochim. Acta, 337 (1999) 163.
15 H. Xia and M. Song, Thermochim. Acta, 429 (2005) 1.
16 N. Delpouve, A. Saiter, J. Mano and E. Dargent, Polymer, 49 (2008) 3130
17 A. Saiter, N. Delpouve, E. Dargent and J. M. Saiter, Eur. Polym. J., 43 (2007) 4675.
18 E. Donth, The Glass Transition, Relaxation Dynamics in Liquids and Disordered Materials, Springer, Berlin 2001, p. 33.
19 E. Dargent, J. Grenet and X. J. Auvray, J. Thermal Anal., 41 (1994) 1409.
20 A. Zumailan, G. Denis, E. Dargent, J. M. Saiter and J. Grenet, J. Therm. Anal. Cal., 68 (2002) 5.
21 E. Gmelin, Thermochim. Acta, 304/305 (1997) 1.
22 I. Fraga, S. Montserrat and J. M. Hutchinson, J. Therm. Anal. Cal., 91 (2008) 687.
23 S. Weyer, A. Hensel and C. Schick, Thermochim. Acta, 305 (1997) 267.
24 J. E. K. Schawe, Thermochim. Acta, 261 (1995) 183.
25 W. Dong, J. Zhao, C. Li, M. Guo, D. Zhao and Q. Fan, Polym. Bull., 49 (2002) 197.
26 A. Leszczynska and K. Pielichowski, J. Therm. Anal. Cal., 93 (2008) 677.
27 C. Lixon, N. Delpouve, A. Saiter, E. Dargent and Y. Grohens, Eur. Polym. J., 44 (2008) 3377.
28 B. Wunderlich, Macromolecular Physics Vol. 3, Academic Press, New York 1980.
29 S. Weyer, M. Merzlyakov and C. Schick, Thermochim. Acta, 377 (2001) 85.
30 P. Slobodian, J. Therm. Anal. Cal., 94 (2008) 545.
31 J. A. Forrest and K. Dalnoki Veress, Adv. Coll. Interf. Sci., 94 (2001) 167.
32 E. Hempel, G. Hempel, A. Hensel, C. Schick and E. Donth, J. Phys. Chem. B, 104 (2000) 2460.
33 R. G. Ferrillo and P. J. Achorn, J. Appl. Polym. Sci., 64 (1997) 191.
34 L. Nunez, M. Villanueva, F. Fraga and M. R. Nunez, J. Appl. Polym. Sci., 74 (1999) 353.
35 W. Brostow, R. Chiu, I. M. Kalogeras and A. Vassilikou-Dova, Matter. Lett., 62 (2008) 3152.
36 N. M. Alves, J. F. Mano and J. L. Gomez Ribelles, Polymer, 43 (2002) 3627.
37 R. A. Talja and Y. H. Roos, Thermochim. Acta, 380 (2001) 109.

ICTAC 2008

DOI: 10.1007/s10973-008-9670-2